arXiv:1605.00867v1 [physics.flu-dyn] 3 May 2016

Weak links between fast mobility and local structure in molecular and atomic liquids

S. Bernini
Dipartimento di Fisica "Enrico Fermi", Università di Pisa, Largo B.Pontecorvo 3, I-56127 Pisa, Italy

F. Puosi
Laboratoire de Physique de l'École Normale Supérieure de Lyon, UMR CNRS 5672, 46 allée d'Italie, 69007 Lyon, France

D. Leporini*
Dipartimento di Fisica "Enrico Fermi", Università di Pisa, Largo B.Pontecorvo 3, I-56127 Pisa, Italy and IPCF-CNR, UOS Pisa, Italy

(Dated: May 4, 2016)

We investigate by Molecular-Dynamics simulations the fast mobility - the rattling amplitude of the particles temporarily trapped by the cage of the neighbors - in mildly supercooled states of dense molecular (linear trimers) and atomic (binary mixtures) liquids. The mixture particles interact by the Lennard-Jones potential. The non-bonded particles of the molecular system are coupled by the more general Mie potential with variable repulsive and attractive exponents in a range which is characteristic of small n-alkanes and n-alcohols. Possible links between the fast mobility and the geometry of the cage (size and shape) are searched. The correlations on a per-particle basis are rather weak. Instead, if one groups either the particles in fast-mobility subsets or the cages in geometric subsets, the increase of the fast mobility with both the size and the asphericity of the cage is revealed. The observed correlations are weak and differ in states with equal relaxation time. Local forces between a tagged particle and the first-neighbour shell do not correlate with the fast mobility in the molecular liquid. It is concluded that the cage geometry alone is unable to provide a microscopic interpretation of the known, universal link between the fast mobility and the slow structural relaxation. We suggest that the particle fast dynamics is affected by regions beyond the first neighbours, thus supporting the presence of collective, extended fast modes.

PACS numbers:
Keywords:

I. INTRODUCTION

Understanding the extraordinary viscous slowing down that characterizes the glass formation is a major scientific challenge [1–3]. From a microscopic point of view, when a liquid approaches the glass transition, the particles are subjected to prolonged trapping by their surroundings and the structural relaxation time τ_α, i.e the average escape time from the cage of the first neighbors, increases from a few picoseconds up to thousands of seconds. During the trapping period the rattling motion inside the cage occurs on picosecond time scales with mean square amplitude $\langle u^2 \rangle$. Henceforth $\langle u^2 \rangle$ will be referred to as "fast mobility". The temporary trapping and subsequent escape mechanisms lead to large fluctuations around the averaged dynamical behavior with strong heterogeneous dynamics [2] and non-exponential relaxation [4]. Pioneering [5, 6] investigations and recent theoretical [7–17] studies addressed the rattling process in the cage to understand the structural relaxation - the escape process - gaining support from numerical [13, 17–41] and experimental works on glassforming liquids [13, 42–45].

Renewed interest about the fast mobility was raised by extensive molecular-dynamics (MD) simulations evidencing the universal correlation between the structural relaxation time τ_α and $\langle u^2 \rangle$ were reported in polymeric systems [29–31], binary atomic mixtures [30, 32], colloidal gels [33] and antiplasticized polymers [13, 35] and compared with the experimental data concerning several glassformers in a wide fragility range ($20 \leq m \leq 191$) [29, 32, 34, 36, 37]. One major finding was that statesof a given physical system, say X and Y, with equal fast mobility $\langle u^2 \rangle$ have equal relaxation times τ_α too:

$$\langle u^2 \rangle^{(X)} = \langle u^2 \rangle^{(Y)} \iff \tau_\alpha^{(X)} = \tau_\alpha^{(Y)} \quad (1)$$

The generalisation of Eq.1 to deal with states of different physical systems is discussed elsewhere [29–32] and exemplified in Sec.III A. After proper account of the molecular-weight dependence Eq.1 extends to longer time scales in polymers where states with equal fast mobility exhibit also equal chain reorientation rate [30, 31] and diffusivity [31, 38]. Correlation between diffusion and fast mobility was observed in atomic mixtures too [32]. A more general relation leading to Eq.1 is provided by the particle displacement distribution, i.e. the incoherent, or self part, of the van Hove function $G_s(r,t)$ [46, 47]. The interpretation of $G_s(r,t)$ is direct. The product $G_s(r,t) \cdot 4\pi r^2 \, dr$ is the probability that the particle is at a distance between r and $r + dr$ from the initial position after a time t. In terms of $G_s(r,t)$ the relation between fast and slow dynamics is expressed by stating that, if two statesof a given physical system are characterized by the *same* displacement distribution $G_s(r,t^*)$ at the trapping time t^*, they also exhibit

*Electronic address: dino.leporini@df.unipi.it

the *same* distribution at long times, e.g. at τ_α [31, 32]:

$$G_s^{(X)}(r,t^*) = G_s^{(Y)}(r,t^*) \iff G_s^{(X)}(r,\tau_\alpha) = G_s^{(Y)}(r,\tau_\alpha) \quad (2)$$

The precise definition of the trapping time t^*(not to be confused with the peak position of the non-Gaussian parameter) will be given in Sec.III A where it will be also shown that Eq.2 implies Eq.1. Actually, the coincidence of the two incoherent van Hove functions extends across all the time interval between t^* and at least τ_α [31, 32]. Eq.2 holds even in the presence of very strong dynamical heterogeneity where both diffusive and jump-like dynamics are observed [31]. From this respect, it offers an interpretation of the scaling of the breakdown of the Stokes-Einstein law in terms of the fast mobility [38] and is consistent with previous conclusions that the long-time dynamical heterogeneity is predicted by the fast heterogeneities [23, 48].

Several approaches suggest that structural aspects matter in the dynamical behavior of glassforming systems. This includes the Adam-Gibbs derivation of the structural relaxation [28, 49] - built on the thermodynamic notion of the configurational entropy [50] -, the mode- coupling theory [51] and extensions [52], the random first-order transition theory [53], the frustration-based approach [54], as well as the so-called elastic models [9, 14–17, 35, 39, 55]. It was concluded that the proper inclusion of many-body static correlations in theories of the glass transition appears crucial for the description of the dynamics of fragile glass formers [56]. The search of a link between structural ordering and slow dynamics motivated several studies in liquids [57–61], colloids [62–64] and polymeric systems [62, 65–70]. We also note that the elastic models of the glass transition conclude that the relaxation is related to the elastic shear modulus, a quantity which is set by the arrangement of the particles in mechanical equilibrium and their mutual interactions [9, 39].

The present work is carried out in the spirit of the cell theory of the liquid state [46]. Each cell is identified by the Voronoi polyhedron (VP) which, as originally suggested by Rahman [6] and later studies [21], provide useful information about the local molecular environment, e.g. to get to the equation of state of the hard sphere liquid [71]. For a given configuration, the VP surrounding a particle encloses all the points which are closer to it than to any other one. Following a preliminary report [72], we investigate by thorough Molecular-Dynamics (MD) simulations the particle fast mobility and relaxation of linear molecules and binary atomic mixtures. The purpose is the assessment of the correlations of the fast mobility $\langle u^2 \rangle$ with the size and the shape of the cage formed by the nearest neighbors of the trapped particle. The local geometry is characterized by the volume and the asphericity of the associated VP. Alternatives are reported [13]. Asphericity has been considered in polymers [13, 21, 72–74], water [21, 75–79] , silica [21], small molecules [75], packed beds of particles [80], hard [81] and soft [82] spheres and its better ability to discriminate different local structures with respect to other features of the Voronoi polyhedron has been noted [80, 82].

The motivation for searching for a connection between cage geometry and fast mobility is that it is intuitively expected. Nonetheless, we find that the correlations are rather weak on a per-particle basis. More insight is provided by grouping the ensemble of particles in (nearly) iso-volume, iso-asphericity and iso-mobility subsets which reveals the increase of the fast mobility in cages with increasing size and asphericity. However, the correlations are weak and differ in states with equal relaxation time, thus preventing the microscopic interpretation of Eq.1, Eq.2 in terms of the cage geometry alone. It is found that the local forces between a tagged particle and the first-neighbour shell do not correlate with the fast mobility in the molecular liquid. We offer arguments suggesting that the single-particle fast mobility is affected by regions extending beyond the nearest neighbours in agreement with other studies [9, 14–17, 23–25, 35, 39, 55, 72, 83–85].

The paper is organized as follows. In Sec. II the MD algorithms are outlined, and the atomic and the molecular models are detailed. The results are presented and discussed in Sec. III. In particular, in Sec. III A the fast rattling motion and the long-time relaxation are characterised, whereas Sec. III B expounds for the first time on the search of cross correlations between the cage geometry and the fast dynamics. Finally, the conclusions are summarized in Sec. IV.

II. METHODS

A. Molecular liquid

A coarse-grained model of fully-flexible linear chains of trimers is used. Nonbonded monomers at a distance r interact via the truncated parametricMie potential [86]:

$$U_{p,q}(r) = \frac{\varepsilon}{q-p}\left[p\left(\frac{\sigma^*}{r}\right)^q - q\left(\frac{\sigma^*}{r}\right)^p\right] + U_{cut} \quad (3)$$

Changing the p and q parameters does not change the position $r = \sigma^* = \sqrt[6]{2}\,\sigma$ and the depth of the potential minimum εbut it affects the fragility of the system [22]. The constant U_{cut} is chosen to ensure $U_{p,q}(r) = 0$ at $r \geq 2.5\,\sigma$. Note that $U_{p,q}(r) = U_{q,p}(r)$. Conventionally $p < q$ and the choice $p = 6, q = 12$ yields the familiar Lennard-Jones (LJ) potential.The Mie potential has been considered to model microscopic interactions in solids including ionic ones ($p = 1$, Born-Mie potential) [87], metallic glasses [88] and polar molecules ($p \simeq 3$), atomic liquids[89], as well as simple and chain molecular [90–92] liquids. We considered the following set of (p, q) pairs: $(7, 15), (8, 12), (7, 11), (6, 12), (6, 8)$. The set, together with the choice of simulating liquids of short trimeric chains, is expected to be characteristic of simple non polar and polar molecular systems. In fact, the optimised parameters (p, q, m_S) of the equation of state for chain molecules formed from m_S tangentially-bonded Mie monomers are [92]: $(6, 18.9, 3)$ for n-decane, $(6, 15.85, 1.96)$ for n-pentane, $(6, 11.7, 2.44)$ for n-butan-1-ol and $(6, 7.61, 1.96)$ for ethanol. Notice that the present work neglects the additional short-ranged square-well potential which is used for the alcohols in ref.[92].

The bonded monomers interact by a potential which is the sum of the LJ potential and the FENE (finitely extended non-

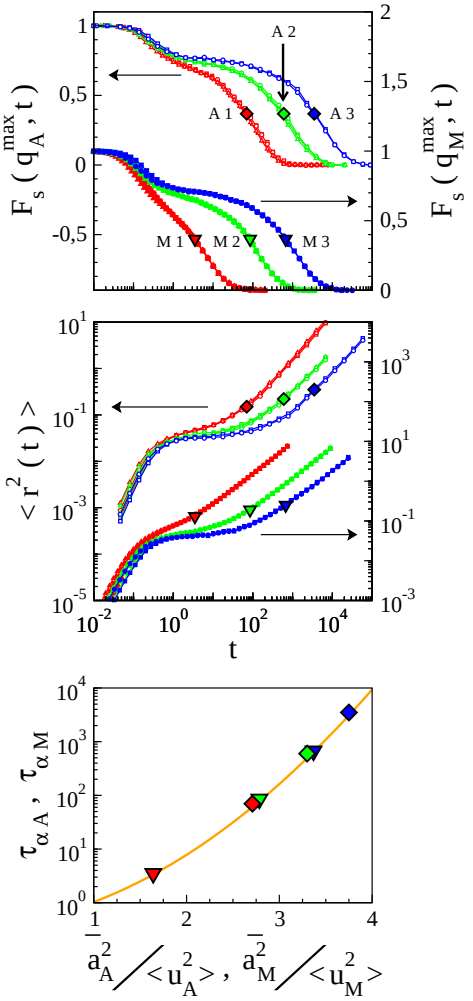

FIG. 1: Top: ISF of selected iso-relaxation time states of the atomic ($A1$, $A2$ $A3$, left axis) and molecular ($M1$, $M2$, $M3$, right axis) liquids. The structural relaxation times of the atomic, $\tau_{\alpha A}$, and molecular, $\tau_{\alpha M}$, liquids are marked as diamonds and triangles, respectively. Middle: corresponding MSD. Note that the MSD of each set of iso-relaxation time states coincide for $t \gtrsim 0.5$, i.e. their fast mobility is equal as stated by Eq.1. Bottom: scaling of the relaxation time and the fast mobility. The continuous line is the master curve given in Eq.3 of ref. [32] ($\overline{a_A^2} = 0.1124$ and $\overline{a_M^2} \equiv \overline{a_P^2} = 0.1243$ [32]). For the atomic liquid the iso-relaxation time states (ρ, T) are: $A1$: □ (1.125,0.388); ○ (1.204,0.55); △ (1.296,0.804). $A2$: □ (1.125,0.338); ○ (1.204,0.48); △ (1.296,0.702). $A3$: □ (1.125,0.317); ○ (1.204,0.45). For the molecular liquid the iso-relaxation time states (ρ, p, q, T) are: $M1$: ■ (1.015,7,15,1); ● (1.070,6,8,0.55); ▲ (1.090,8,12,1.35). $M2$: ■ (1.018,7,15,0.7); ● (1.070,6,8,0.39); ▲ (1.1,7,11,0.79). $M3$: ■ (0.984,6,12,0.33); ● (1.086,6,12,0.63).

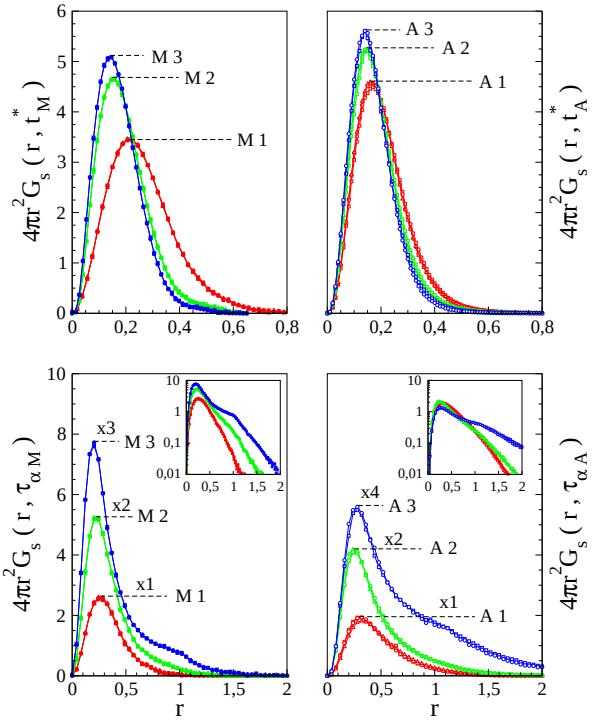

FIG. 2: Incoherent van Hove function of the iso-relaxation time states evaluated at the trapping (top) and the structural relaxation (bottom) times of the molecular (left) and the atomic (right) liquids. The figure evidences the strong version of the scaling between the fast trapping regime and the slow relaxation one (Eq.2). Note that $G_s(r, \tau_\alpha)$ of the sets of states M3 and A3 exhibits a bump at $r \sim 1$, the particle diameter, due to the jump dynamics characteristic of slowed-down states. The insets show that the coincidence of $G_s(r, \tau_\alpha)$ extends to regions where the exponential tails related to the dynamic heterogeneity are apparent [93].

linear elastic) potential [94]:

$$U_{FENE}(r) = -\frac{1}{2} k R_0^2 \ln\left(1 - \frac{r^2}{R_0^2}\right) \qquad (4)$$

where k measures the magnitude of the interaction and R_0 is the maximum elongation distance. The parameters k and R_0 have been set to $30\,\varepsilon/\sigma^2$ and $1.5\,\sigma$ respectively [95]. The resulting bond length is $b = 0.97\sigma$ within a few percent. All quantities are in reduced units: length in units of σ, temperature in units of ε/k_B and time τ_{MD} in units of $\sigma\sqrt{\mu/\varepsilon}$ where μ is the monomer mass. We set $\mu = k_B = 1$.

We study systems of $N_M = 2001$ monomers at different density ρ, temperature T and p, q parameters. Each state is labeled by the multiplet (ρ, p, q, T). For clarity reasons, the details about the states are given in the caption of Fig. 1.

NVT ensemble (constant number of particles, volume and temperature) has been used for equilibration runs, while NVE ensemble (constant number of particles, volume and energy) has been used for production runs for a given state point. NVT ensemble is studied by the extended system method introduced by Andersen [96] and Nosé [97]. The numerical integration of the augmented Hamiltonian is performed through the multiple time steps algorithm, reversible Reference System Propagator Algorithm (r-RESPA) [98].

It is interesting to map the reduced MD units to real physical units. The procedure involves the comparison of the experiment with simulations and provide the basic length σ, temperature ε/k_B and time τ_{MD} units [94, 99–102]. For example

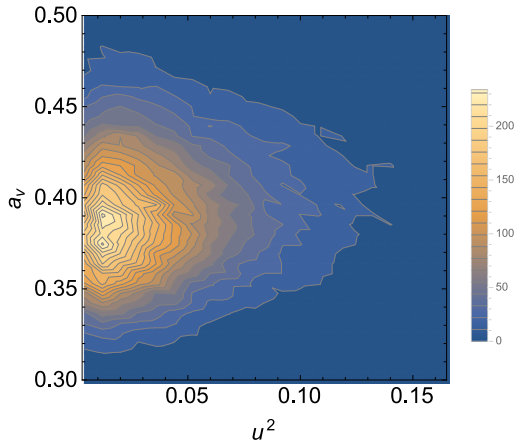

FIG. 3: Joint distribution of the VP asphericity a_v and the fast mobility u^2, $P(a_v, u^2)$, of the molecular-liquid state ● (see caption of Fig. 1). The two small peaks at $u^2 \simeq 0.012$ with $a_v \simeq 0.375$ and $a_v \simeq 0.39$ are the peaks of the distributions of the central (higher asphericity) and the end (lower asphericity) monomers of each chain. Note that the peaks occurs virtually at the same fast mobility u^2, i.e. the different cage asphericities do not lead to different mobilities.

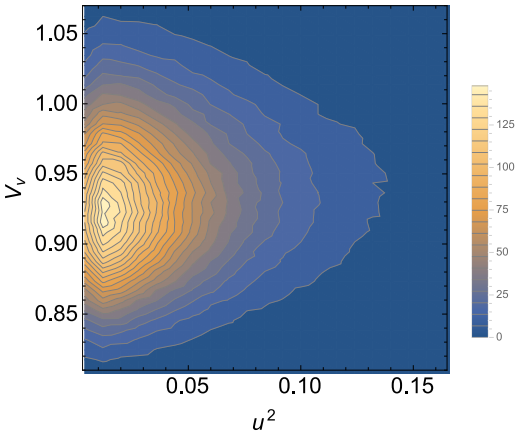

FIG. 4: Joint distribution of the VP volume V_v and the fast mobility u^2, $P(V_v, u^2)$, of the molecular-liquid state state ● (see caption of Fig. 1). The two small peaks at $u^2 \simeq 0.012$ with $V_v \simeq 0.915$ and $V_v \simeq 0.93$ are the peaks of the distributions of the central and the end monomers of each chain, respectively [105]. Note that the peaks occurs at the same fast mobility u^2, i.e. the different volumes do not result in different mobilities.

for polyethylene and polystyrene it was found $\sigma = 5.3$ Å, $\varepsilon/k_B = 443$ K ,$\tau_{MD} = 1.8$ ps and $\sigma = 9.7$ Å, $\varepsilon/k_B = 490$ K ,$\tau_{MD} = 9$ ps respectively [100].

B. Binary atomic mixture

An 80:20 binary mixture of $N_{BM} = 4000$ particles is considered [103]. The two species A, B interact via the potential:

$$U_{\alpha,\beta}(r) = \varepsilon_{\alpha,\beta}\left[\left(\frac{\sigma^*_{\alpha,\beta}}{r}\right)^{12} - 2\left(\frac{\sigma^*_{\alpha,\beta}}{r}\right)^{6}\right] + U_{cut} \quad (5)$$

which is similar to Eq. 3 with $p = 6, q = 12$ except that the height and the minimum of the potential now depend on the interacting species, being $\alpha, \beta \in \{A, B\}$ with $\sigma_{AA} = 1.0$, $\sigma_{AB} = 0.8$, $\sigma_{BB} = 0.88$, $\varepsilon_{AA} = 1.0$, $\varepsilon_{AB} = 1.5$, $\varepsilon_{BB} = 0.5$. We set the masses $m_A = m_B = 1$. Using argon units for the A particles $\sigma_{AA} = 3.405$ Å, $\varepsilon_{AA}/k_B = 119.8K$, $m_A = 6.6337 \cdot 10^{-26}$ Kg, the time unit is $\tau'_{MD} = (\sigma^2_{AA} m_{AA}/\varepsilon_{AA})^{1/2} = 2.2$ ps [104]. The system is equilibrated in the NTV ensemble and the production runs are carried out in the NVE ensemble. NTV runs use a standard and Nosé method [97]. The "velocity verlet" integration algorithm is used both in the NVE and NVT ensembles. We investigate only the A particles of states with different number density ρ and temperature T. Each state is labeled by the multiplet (ρ, T). For clarity reasons, the details about the states are given in the caption of Fig. 1.

III. RESULTS

A. Fast mobility and relaxation

We consider the mean square displacement, i.e. the second moment of the incoherent van Hove function:

$$\langle r^2(t)\rangle = 4\pi \int_0^\infty r^2 G_s(r,t)\, r^2 dr \quad (6)$$

At short times it is known that the derivative $\Delta(t) = \partial \log\langle r^2(t)\rangle / \partial \log t$ exhibits a minimum at $t = t^*$ [29, 30, 32]. t^* is a measure of the trapping time of the particle and, in actual units, corresponds to a few picoseconds. In the present molecular liquid model, $t^*_M \cong 1$ and it is virtually independent of the physical state [29, 30]. Instead, in the binary mixture t^*_A and t^*_B increase slightly with the relaxation time [30, 32]. We define the fast mobility of the monomers of the linear chains ($i = M$) and the A particles of the atomic mixture ($i = A$) as the short-time mean square displacement:

$$\langle u_i^2\rangle = \langle r^2(t = t_i^*)\rangle, \qquad i \in \{A, M\} \quad (7)$$

The fast mobility is the mean square amplitude of the position fluctuations of the tagged particle in the cage of the neighbours. The B particles are not considered. Henceforth, the i subscript is removed from $\langle u_i^2\rangle$ for clarity reasons, leaving the identification to the context.

With the purpose of characterizing the long-time structural relaxation we consider the incoherent, self-part of the intermediate scattering function [47]:

$$F_s(q,t) = \int G_s(\boldsymbol{r},t)\exp(-i\boldsymbol{q}\cdot\boldsymbol{r})\, d\boldsymbol{r} \quad (8)$$

$$= 4\pi \int_0^\infty G_s(r,t)\,\frac{\sin qr}{qr}\, r^2 dr \quad (9)$$

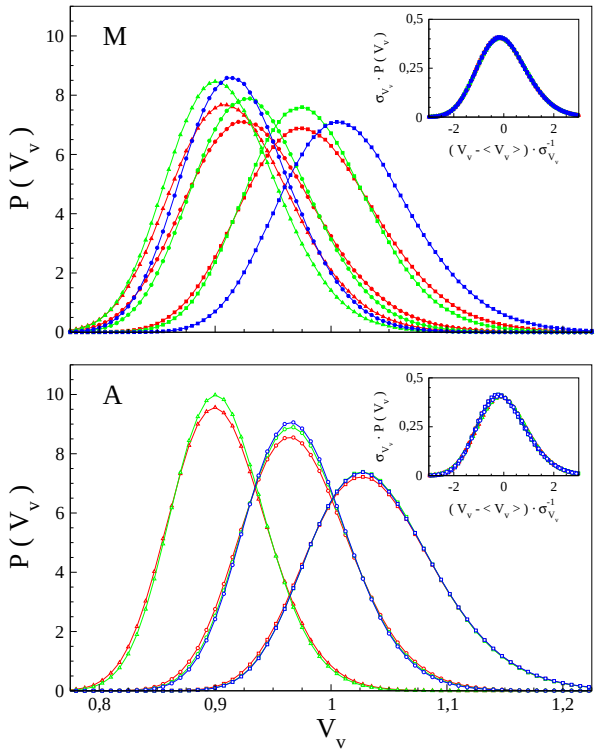

FIG. 5: Distribution of the VP volume V_v of the iso-relaxation time states of the molecular (top) and the atomic (bottom) liquids considered in Fig.1 (same symbols and color codes). It is seen that states with *equal* relaxation time have *different* distributions. The inserts show that the distributions collapse to a single master curve by proper shift and scaling in terms of their average and standard deviation, respectively.

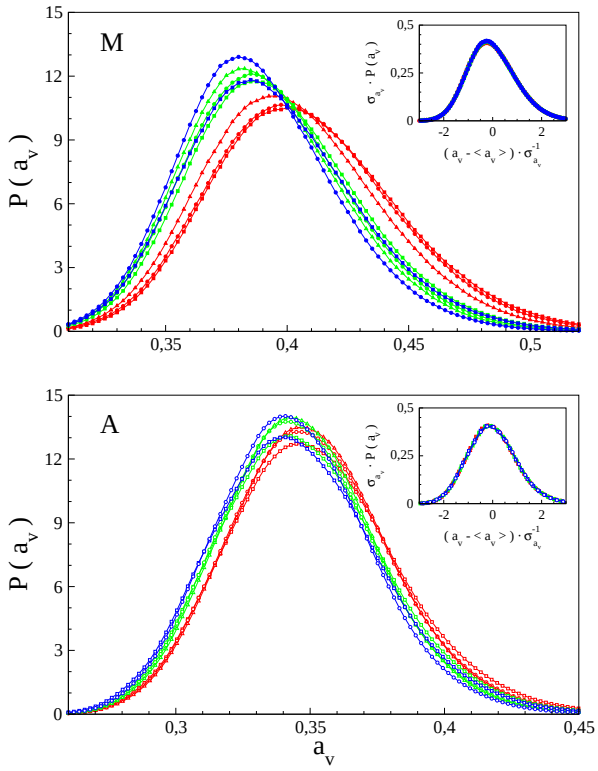

FIG. 6: Distribution of the VP asphericity a_v of the iso-relaxation time states of the molecular (top) and the atomic (bottom) liquids considered in Fig.1 (same symbols and color codes). It is seen that states with *equal* relaxation time have *different* distributions. The inserts show that the distributions collapse to a single master curve by proper shift and scaling in terms of their average and standard deviation, respectively.

Eq.9 follows from the isotropy of the liquids. The intermediate scattering function provides a convenient function to study the rearrangements of the spatial structure of the fluid over the length scale of $2\pi/q$. $F_s(q,t)$ is evaluated at the maximum of the static structure factor, $q = q^{max}$, with $7.02 \leq q_M^{max} \leq 7.39$ for the molecular liquid and $7.05 \leq q_A^{max} \leq 7.38$ for the A particles of the atomic mixture. We are interested in the structural relaxation of the molecular liquid ($i = M$) and the A fraction of the binary mixture ($i = A$) and define the structural relaxation time by the equation:

$$F_s(q_i^{max}, \tau_{\alpha i}) = e^{-1} \quad i \in \{A, M\} \tag{10}$$

According to Eq.6, Eq.7, Eq.8 and Eq.10, two states X and Y fulfilling Eq. 2 exhibit *equal* fast mobility and *equal* relaxation times, i.e. Eq.1.

Selected groups of iso-relaxation time states will be now characterized. They are labelled as $M1$, $M2$, $M3$ and $A1$, $A2$, $A3$ and refer to the molecular and the atomic liquids, respectively. Details about the states are included in the caption of Fig. 1 which shows their intermediate scattering function (top) and mean square displacement (middle). It is seen that, after the ballistic regime, the mean square displacement of each set of iso-relaxation time states coincide for $t \gtrsim 0.5$, i.e. their fast mobility is equal as stated by Eq.1. The bottom panel of Fig.1 shows that the iso-relaxation time states agree with the scaling between the relaxation and the fast mobility [29–32].Note that a unique master curve encompasses both the atomic and the molecular system. Fig.1(bottom) illustrates the scaling procedure of the fast mobility to extend Eq.1 and deal with states of different physical systems. The procedure is widely discussed elsewhere [29–32].

Fig. 2 plots the incoherent van Hove function $G_s(r,t)$ at the trapping (top) and the relaxation times (bottom). It evidences the strong version of the scaling between the fast trapping regime and the slow relaxation one, as stated by Eq.2, namely it shows that the coincidence of the incoherent van Hove function $G_s(r,t)$ at $t = \tau_\alpha$ of the iso-relaxation time states implies the coincidence at the trapping time $t = t^*$ as well. The coincidence of $G_s(r,t^*)$ implies the coincidence of the distributions of the fast mobilities in that:

$$P(u^2) = 2\pi\sqrt{u^2}\, G_s\left(\sqrt{u^2}, t^*\right) \tag{11}$$

Note that: i) $G_s(r,\tau_\alpha)$ of the set of states $M3$ and $A3$ exhibits the characteristic bump of the jump dynamics at $r \sim 1$ (the particle diameter) and ii) the coincidence of $G_s(r,\tau_\alpha)$ includes the exponential tails due to the dynamic heterogeneity

[93] (see insets of Fig. 2). This makes it apparent that the fast caged dynamics is enough to predict key aspects of the dynamical heterogeneity of the glass formers [106], as also seen by previous studies of the breakdown of the Stokes-Einstein law [38] and the non-gaussian character of the particle displacements [107].

B. Correlations between cage geometry and fast mobility

To characterize the geometry of the cages of the particles, we perform a Voronoi tessellation. In particular, we are interested in both the volume V_v and the asphericity a_v of VPs. The asphericity is defined as:

$$a_v = \frac{(A_v)^3}{36\pi\,(V_v)^2} - 1 \tag{12}$$

where A_v is the VP surface. The asphericity vanishes for a spherical VP and is positive otherwise.

Our search of the possible correlation between the cage geometry and the fast mobility considers the *initial* volume V_v and asphericity a_v of the VP surrounding a particle at time t_0, and compute the *subsequent* square displacement of the particle between t_0 and $t_0 + t^*$, u^2. The ensemble average of u^2 coincides with Eq.7.

1. *Joint distributions $P(a_v, u^2)$ and $P(V_v, u^2)$*

First, the joint probability distribution $P(X, u^2)$ with $X \in \{a_v, V_v\}$ is examined. The distribution is found to be negligibly dependent on the physical state and the kind of system, molecular or atomic liquid.

As an example, Fig. 3 shows the probability distribution $P(a_v, u^2)$ for one state of the molecular liquid. The average is $\langle a_v \rangle \simeq 0.39$ which is close to the one of a dodecahedron ($a_v = 0.325034$), namely the cage asphericity is small as a consequence of the good packing of the particles. Fig. 3 strongly suggests that the correlation between the fast mobility u^2 of the particle and the cage asphericity is rather poor on a per-particle basis. This is not due to the "myopic" spatial resolution of $P(a_v, u^2)$. In fact, there is clear evidence of two peaks located at $u^2 \simeq 0.012$ and $a \simeq 0.38$ which are seen to correspond (not shown) to the peaks of the distribution $P(a_v, u^2)$ restricted to the inner (higher asphericity) and the end (lower asphericity) monomers. Fig.4 shows the probability distribution $P(V_v, u^2)$ for the same state of the molecular liquid. The pattern is very similar to the one of $P(a_v, u^2)$. In particular, the peaks of the distributions of the central (smaller volume) and the end (larger volume) monomers of each chain are seen [105].

The double-peak structure of both Fig. 3 and Fig.4 shows that the inner and the end monomers of the chain molecule have *equal* fast mobility in spite of the *different* size [105] and shape of their cages (see also Fig.6 of ref.[72]). This suggests, in addition to the poor correlations seen in Fig. 3 and Fig.4, that the fast mobility is not driven only by the geometry of the cage. This aspect will be discussed in the next sections in more detail.

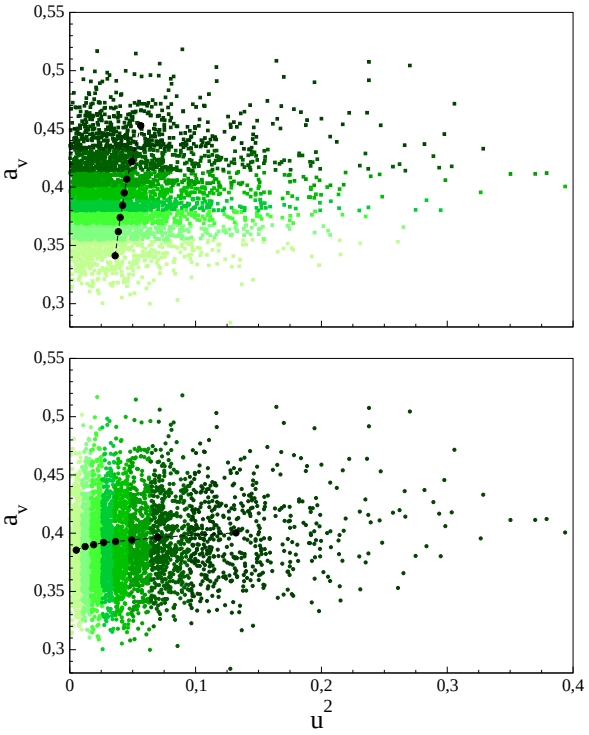

FIG. 7: Subset partition of one ensemble of realisations of the fast mobility-asphericity pairs $\{u^2, a_v\}$ of the molecular-liquid state ● (see caption of Fig. 1). Top: asphericity subsets; the black dots have coordinates $\{\langle u^2\rangle_{a_v,s}, \langle a_v\rangle_{a_v,s}\}$ with $s = 1, \cdots, 8$. $\langle u^2\rangle_{a_v,s}$ and $\langle a_v\rangle_{a_v,s}$ are the averages of the fast mobility and the asphericity restricted to each set, i.e. Eq.15 and Eq.16 with $X = Z = a_v$, respectively. Bottom: fast-mobility subsets; the black dots have coordinates $\{\langle u^2\rangle_{u^2,s}, \langle a_v\rangle_{u^2,s}\}$ with $s = 1, \cdots, 8$. $\langle u^2\rangle_{u^2,s}$ and $\langle a_v\rangle_{u^2,s}$ are the averages of the fast mobility and asphericity restricted to each set, i.e. Eq.15 and Eq.16 with $X = a_v$, $Z = u^2$, respectively. Note that the average mobility increases with the average asphericity in both kinds of partitions.

2. *Marginal distributions $P(a_v)$ and $P(V_v)$ of iso-relaxation states*

The previous section shows that the joint distribution of the *initial* local geometry and the *subsequent* fast dynamics of a single state does not reveal clear correlations. This suggests the limited insight provided by the per-particle analysis. To substantiate the matter, we compare the states with equal relaxation time, and then equal average global fast mobility according to Eq.1, which are shown in Fig.1 and Fig. 2. Clear indications are drawn by examining the marginal distributions of the VP volume and asphericity, $P(V_v)$ and $P(a_v)$ respectively:

$$P(X) = \int P(X, u^2)\, du^2, \qquad X \in \{V_v, a_v\} \tag{13}$$

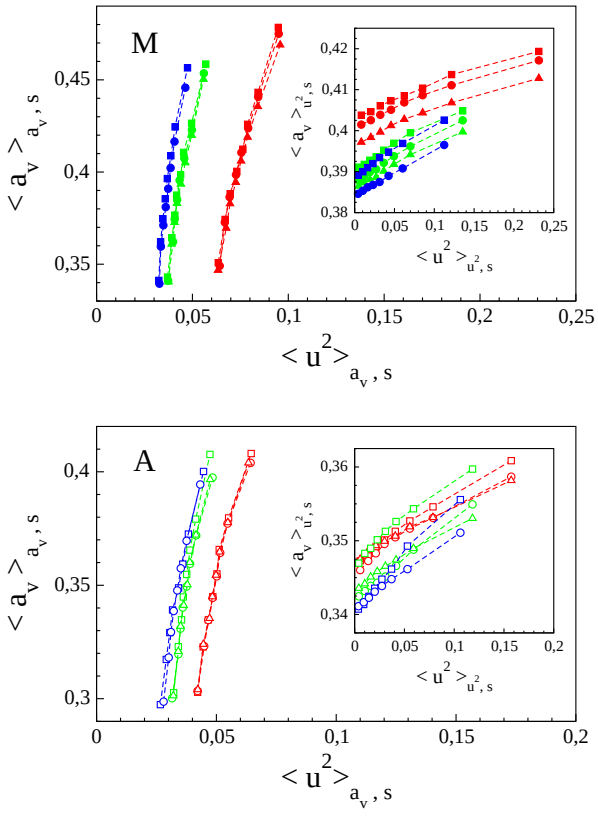

FIG. 8: Relation between the initial average asphericity and the subsequent average fast mobility of the particles belonging to the asphericity subsets (see Fig. 7 top). Particles are the monomers of the molecular liquid (top) and the A particles of the atomic mixture (bottom). The inserts plot the same relation for the fast-mobility subsets (see Fig. 7 bottom). In both kind of subsets the mobility increases with the cage asphericity in a state-dependent way. Symbols and color codes as in Fig.1.

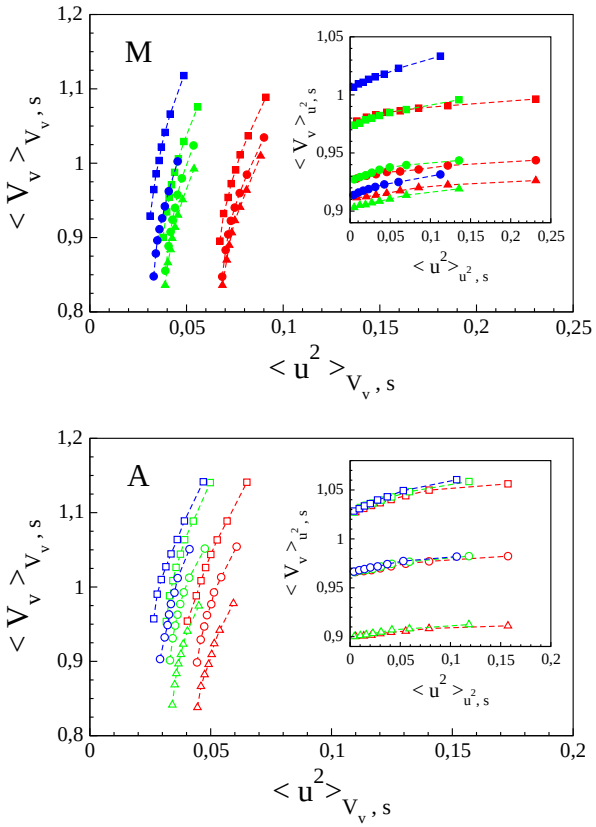

FIG. 9: Relation between the initial average cage volume and the subsequent average fast mobility of the particles belonging to the volume subsets. Particles are the monomers of the molecular liquid (top) and the A particles of the atomic mixture (bottom). The inserts plot the same relation for the fast-mobility subsets. In both kind of subsets the mobility increases with the cage asphericity in a state-dependent way. Symbols and color codes as in Fig.1.

Fig. 5 plots the distributions of the VP volume of the monomers of the molecular liquid (top) and the A particles of the binary mixtures (bottom). It is seen that states with *equal* relaxation time have *different* distributions. The differences are traced back to differences in the average VP volume $(1/\rho)$ and variance. If they are removed by proper scaling, the shape of the distributions coincide (see inserts),thus confirming previous claims about its universality [21]. Fig. 5 suggests that the VP volume is a poor predictor of the long-time relaxation. The weak correlations between the VP volume and the dynamics has been already noted in polymers [21].

Fig. 6 plots the distributions of the VP asphericity of the monomers of the molecular liquid (top) and the A particles of the binary mixtures (bottom). Some similarities with the volume distributions are apparent, namely: i) the distributions depend on the state and are *different* even if the states have *equal* relaxation time, ii) the different distributions collapse on a master curve by proper scaling in terms of the average and the variance (see inserts),thus confirming previous claims about its universality [21]. The asphericity distribution depends on the state but the changes are much more limited than the ones of the VP volume, especially as far as the atomic mixture is concerned, due to the good packing. The limited asphericity changes must be contrasted with the wide changes of the structural relaxation time (Fig.1). We point out that the average asphericity is higher for the molecular liquid than the atomic mixture. This is ascribed to the bonds of the molecule. In fact, the cage surrounding a monomer is less spherical due to the presence of one or two other bonded monomers which are closer than the non-bonded monomers (see Sec. II)[108].

3. *Subset distributions of iso-relaxation states*

According to Sec.III B 1 and Sec.III B 2, looking at the systems on particle-by-particle basis does not identify links between the rattling of a particle confined by the first neighbours and the cage geometry.

We now show that more insight is drawn by grouping fast mobility and local geometries in subsets. To this aim, we partition the distributions $P(X, u^2)$ with $X \in \{a_v, V_v\}$ in subsets taken as octiles. We consider two different kinds of sub-

sets: stripes parallel to the u^2 axis, resulting in volume or asphericity subsets and stripes parallel to the X axis resulting in fast-mobility subsets. Fig.7 provides an illustrative example of the two kinds of partitions with $X = a_v$. In general, the s-th stripe $[Z_s, Z_{s+1}]$, $Z \in \{a_v, V_v, u^2\}$, is defined as:

$$\int_{[Z_s,Z_{s+1}]} P(X,u^2)\,dX\,du^2 = \frac{1}{8}, \quad s = 1,\cdots,8 \tag{14}$$

with $Z_1 = 0, \cdots, Z_9 = \infty$. The relevant averages restricted to the s-th Z stripe are defined as ($X \in \{a_v, V_v\}$) :

$$\langle u^2\rangle_{Z_s} = 8\int_{[Z_s,Z_{s+1}]} u^2\,P(X,u^2)\,dX\,du^2 \tag{15}$$

$$\langle X\rangle_{Z_s} = 8\int_{[Z_s,Z_{s+1}]} X\,P(X,u^2)\,dX\,du^2 \tag{16}$$

Both $\langle u^2\rangle_{Z_s}$ and $\langle X\rangle_{Z_s}$ increase $s = 1,\cdots,8$. As an example, Fig.7 shows the location of the points $\{\langle u^2\rangle_{a_v,s}, \langle a_v\rangle_{a_v,s}\}$ (top) and $\{\langle u^2\rangle_{u^2,s}, \langle a_v\rangle_{u^2,s}\}$ (bottom). By definition, the relation between the global and the subset averages is:

$$\langle \Re\rangle = \frac{1}{8}\sum_{s=1}^{8}\langle \Re\rangle_{Z_s} \tag{17}$$

Similar divisions in subsets were carried out in previous studies too. The partition of local structures in subsets according to the VP asphericity has been considered for characterising the water structure [76] , whereas the correlations between the VP volume and the displacements of the fastest and the slowest particles were investigated in colloids and polymers [62].

First, we investigate all the states in terms of the asphericity and the fast-mobility subsets (for illustration see Fig. 7). Fig. 8 plots the *initial* average asphericity of the cage versus the *subsequent* average fast mobility of the two classes of subsets. It is seen that the mobility increases with the cage asphericity. There is no clear signature of this intuitive result in Fig.3. This is due to the weak correlations which manifest in Fig. 8. In fact, $\langle u^2\rangle_{a_v,s}$ is weakly dependent on $\langle a_v\rangle_{a_v,s}$ (Fig. 8, main panels), and $\langle a_v\rangle_{u^2,s}$ is weakly dependent on $\langle u^2\rangle_{u^2,s}$ (Fig. 8, inserts).

The subset analysis is now applied to the cage size. Fig. 9 summarizes the results concerning the volume and the fast-mobility subsets as a plot of the *initial* average volume of the cage versus the *subsequent* average fast mobility. It is seen that the mobility increases with the cage size in both kind of subsets. Similarly to the asphericity, there is no clear signature of this second intuitive result in Fig.4 due to the weak correlations. The weak increase of the mobility with the VP volume has been also noted in colloids and polymers by considering the displacements of 10 % fastest and 10 % slowest particles [62]. All in all, Fig. 9 confirms that the VP volume is of modest interest [21, 109].

One disappointing conclusion drawn by both Fig.8 and Fig.9 is that the increase of the mobility with either the cage size or asphericity is *state dependent*. In particular, the increase is different even if the states have equal relaxation time. Such states have identical distribution of the fast mobility, Eq.11. Then, if X and Y are two iso-relaxation states, one has from Eq.15:

$$\langle u^2\rangle^{(X)}_{u^2,s} = \langle u^2\rangle^{(Y)}_{u^2,s}\,, \quad s = 1,\cdots,8 \tag{18}$$

Eq.18 states that, if the states have equal relaxation time, the fast-mobility subsets have *equal* average value of the fast mobility. Nonetheless, the inserts of Fig.8 and Fig.9 show that the *initial* average size and shape of the cages embedding these particles are *different*.

As a final remark, we remind that both the fast mobility $\langle u^2\rangle$ and the structural relaxation time have relation with the voids between particles, as measured by the Positron Annihilation Lifetime Spectroscopy (PALS) [110]. Recently, it was shown that $\langle u^2\rangle \propto \tau_3$ where τ_3 is the PALS lifetime, which is related to the average size of the cavity where the annihilation takes place [36, 37]. Our findings about the poor correlation between the fast mobility and the cage size are seemingly at variance with this experimental results. However, it must be noted that PALS is sensitive to the *unoccupied volume* which is more closely represented by the volume of the tetrahedra following the Delaunay tessellation [111]. Our study is concerned with the Voronoi tessellation. The difference between the two tessellations is that the Delaunay tetrahedron describes the shape of the cavity between the particles whereas the Voronoi polyhedron describes the coordination of the nearest-particles. The investigation of the possible correlation between the fast mobility and the size/ shape of the Delaunay tetrahedra is beyond the purpose of the present paper.

4. *Fast mobility and local forces*

Ultimately, the mobility of a tagged particle is set, in addition to kinetic aspects, by the total force $\mathbf{F}$ exerted by the surroundings which, in turn, depends on the geometry of the particles arrangement *and* the interaction potential. Our present results point to the conclusion that the *local* geometry correlates poorly with the fast mobility. In order to understand if, in spite of the minor role of the cage geometry, states with identical fast mobility exhibit common aspects of the total force acting on a particle, we investigated the distribution of the modulus $P(F)$ [112]. In particular, we are interested in the mean square force (MSF) $\langle F^2\rangle$ which includes both binary and triplet force contributions [113]. MSF is related to the second frequency moment of the velocity correlation function Ω_0^2 :

$$\langle F^2\rangle = 3m\,k_B\,T\,\Omega_0^2 \tag{19}$$

m being the particle mass [113]. Ω_0 is largely contributed by local forces, i.e. the ones between the tagged particle and the first-neighbour shell, [113] and represents the frequency at which the tagged particle would vibrate if it were undergoing small oscillations in the potential well produced by the surrounding particles when kept fixed at their mean equilibrium positions around the tagged particle [47]. Then, the ratio $\langle F^2\rangle\,\sigma^2/k_B^2T^2 = \langle F^2\rangle/T^2$ is a measure of the local stiffness.

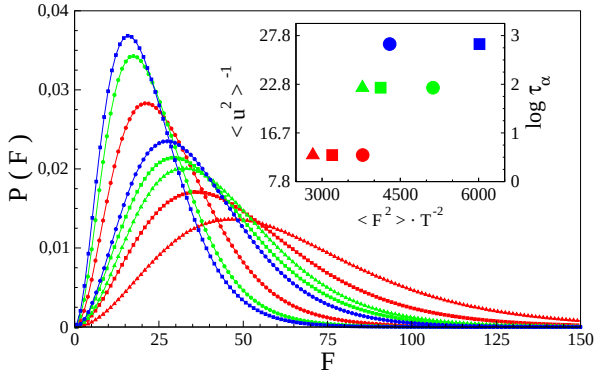

FIG. 10: Distribution of the total force acting on a particle of the molecular liquid in the three different sets of states of Fig.1 with equal fast mobility. The inset shows the poor correlation between the fast mobility of the same states with the local stiffness.

Fig. 10 shows that states of the molecular liquid with equal fast mobility have quite different distributions of the total force. They also exhibit different local stiffness (Fig. 10, inset). Note also that states with rather different relaxation times have rather similar local stiffness. Even if other states, in particular much closer to the glass transition, should be investigated to provide wider evidence, we preliminarily conclude that the fast mobility in a mildly-supercooled *molecular* liquid is not driven by the force exerted by the closest neighbours. Notice that iso-mobility and iso-relaxation time states of an *atomic* liquid, with equal density and temperature, exhibit identical local force distributions $P(F)$, and then equal MSF [112]. This different behaviour needs further investigation.

5. *Why poor correlations ?*

The present study reaches three major conclusions:

- there are weak correlations between fast mobility, i.e. the rattling of the particle trapped by the cage of the neighbours, and the cage geometry itself.
- the cage geometry is unable to provide a microscopic interpretation of the correlation between the cage rattling and the slow structural relaxation as expressed by Eq.1, Eq.2. In fact, it is found that two iso-relaxation states have quite clear correlations between their fast dynamics, but no obvious relations between their cage geometries.
- local forces between a tagged particle and the first-neighbour shell do not correlate with the fast mobility in mildly supercooled states of the molecular liquid.

Why these failures ? Our results must not lead to the conclusion that no correlation between the structure and the dynamics exists, in that the coupling between the dynamic and the structure is reported in the atomic mixture [85] and the molecular liquid [94] under study, also due to the harsh short-ranged repulsive character of the potentials. Instead, we notice that the VP volume and asphericity are mainly controlled by the closest neighbours of the particle and then poorly sensitive to the liquid structure beyond the first shell. This aspect matters. The influence of structure on dynamics is much stronger on long length scales than on short ones in the atomic mixture [85].

Furthermore, there are evidences in the molecular liquid studied here that the fast motion follows from the collective motion of regions extending more than the first coordination shell, a finding which is consistent with elastic models [9, 14–17, 23–25, 35, 39, 55, 83]. One piece of evidence comes from the identical fast mobility of *separate* parts of the molecule, i.e. the end and the central monomers of the molecule, irrespective of the different asphericity and size of their cages, see Fig. 3 and Fig.4 of the present paper, as well as Fig.6 of ref.[72] where the same result is found in much longer chain molecules. Furthermore, it has been evidenced that a given monomer and the surrounding particles up to the next-next-nearest neighbours undergo *simultaneous*, *correlated*, rapid displacements within the trapping time t^* over which the fast mobility is evaluated (see Eq.7) [40, 41]. One appealing feature of the correlations between the fast displacements is that both their *strength* and *spatial extension* are *identical* in states with *equal* relaxation time and increase with the latter, thus suggesting non-local interpretations of the link between the cage rattling and the slow structural relaxation (Eq.1, Eq.2) [40, 41]. The non-local view is in harmony with the finding that the structural relaxation does not correlate with the infinite-frequency elastic response, which is *local* in nature, but with the *quasi-static* elastic response at zero wavevector (k=0) which occurs under *mechanically equilibrium* ($\mathbf{F} = 0$) [39, 55]. This has important implications. In fact, the deformation field at low frequency is quite extended and, indeed, is scale-free in simple examples , e.g. it decays as r^{-x} with $x = 1$ for a localised force and $x = 2$ for cavity expansion.

The suggested presence of non-local fast collective motion agrees with the evidence of quasi-local soft modes, i.e. with an extended component, in MD simulations of 2D binary mixtures and the finding that the regions of motion of the quasi-local soft modes exhibit striking correlation with the regions of high Debye-Waller factor [23–25]. Moreover, it has been proposed that structural relaxation in deeply supercooled liquids proceeds via the accumulation of Eshelby events, i.e. local rearrangements that create long-ranged and anisotropic stresses in the surrounding medium [84].

IV. CONCLUSIONS

The present MD study aims at clarifying the role of the cage geometry in affecting the fast mobility $\langle u^2 \rangle$, namely the rattling amplitude of the particles temporarily trapped by the cage of the neighbors, in mildly supercooled states. The fast mobility is a very accurate predictor of the long-time relaxation, as summarized by Eq.1, stating that two states with equal fast mobility have equal relaxation time as well [13, 29–

34, 36–38, 40, 41], and the more general Eq.2 linking the single-particle fast dynamics and slow relaxation [31, 32]. The cage geometry has been characterised by the volume V_v and the asphericity a_v of the Voronoi polyhedra following the tessellation of the configurations of both a molecular and an atomic liquid. A novel cross-correlation analysis between the fast mobility and the Voronoi volume and shape has been performed.

Signatures of connection between the fast mobility and the cage geometry are not found in either the joint ($P(a_v, u^2)$ and $P(V_v, u^2)$) or the marginal ($P(a_v)$ and $P(V_v)$) distributions. Weak correlations are identified by partitioning the Voronoi cells in asphericity and size subsets, as well as by dividing the particles in fast-mobility subsets. The procedure reveals the increase of the average fast-mobility with the average size and asphericity of the different subsets. The observed correlations are not the same in states with equal relaxation time, leading us to the conclusion that the cage geometry is unable to provide a microscopic interpretation of the link between the cage rattling and the slow structural relaxation, as expressed by Eq.1, Eq.2. Local forces between a tagged particle and the first-neighbour shell do not correlate with the fast mobility in the molecular liquid. We suggest that the single-particle fast mobility follows by modes extending beyond the first neighbours.

Acknowledgments

A generous grant of computing time from IT Center, University of Pisa and M. Righini, ®Intel is gratefully acknowledged.

[1] P. G. Debenedetti and F. H. Stillinger, Nature **410**, 259 (2001).
[2] L. Berthier and G. Biroli, Rev. Mod. Phys. **83**, 587 (2011).
[3] M. D. Ediger and P. Harrowell, J. Chem. Phys. **137**, 080901 (2012).
[4] C. Monthus and J.-P. Bouchaud, J. Phys. A: Math. Gen. **29**, 3847 (1996).
[5] A. Tobolsky, R. E. Powell, and H. Eyring, in *Frontiers in Chemistry*, edited by R. E. Burk and O. Grummit (Interscience, New York, 1943), vol. 1, pp. 125–190.
[6] A. Rahman, J. Chem. Phys. **45**, 2585 (1966).
[7] C. A. Angell, Science **267**, 1924 (1995).
[8] R. W. Hall and P. G. Wolynes, J. Chem. Phys. **86**, 2943 (1987).
[9] J. C. Dyre, Rev. Mod. Phys. **78**, 953 (2006).
[10] L.-M. Martinez and C. A. Angell, Nature **410**, 663 (2001).
[11] K. L. Ngai, Phil. Mag. **84**, 1341 (2004).
[12] K. L. Ngai, J. Non-Cryst. Solids **275**, 7 (2000).
[13] D. S. Simmons, M. T. Cicerone, Q. Zhong, M. Tyagic, and J. F. Douglas, Soft Matter **8**, 11455 (2012).
[14] L. Yan, G. Düring, and M. Wyart, PNAS **110**, 6307 (2013).
[15] S. Mirigian and K. S. Schweizer, J. Chem. Phys. **140**, 194506 (2014).
[16] S. Mirigian and K. S. Schweizer, J. Chem. Phys. **140**, 194507 (2014).
[17] F.Puosi and D.Leporini, arXiv:1108.4629v2.
[18] C. A. Angell, J. Am. Chem. Soc. **86**, 117 (1968).
[19] S.V.Nemilov, Russ. J. Phys. Chem. **42**, 726 (1968).
[20] J. Shao and C. A. Angell, in *Proc. XVIIth International Congress on Glass, Beijing* (Chinese Ceramic Societ, 1995), vol. 1, pp. 311–320.
[21] F. Starr, S. Sastry, J. F. Douglas, and S. Glotzer, Phys. Rev. Lett. **89**, 125501 (2002).
[22] P. Bordat, F. Affouard, M. Descamps, and K. L. Ngai, Phys. Rev. Lett. **93**, 105502 (2004).
[23] A. Widmer-Cooper and P. Harrowell, Phys. Rev. Lett. **96**, 185701(4) (2006).
[24] A. Widmer-Cooper, H. Perry, P. Harrowell, and D. R. Reichman, Nature Physics **4**, 711 (2008).
[25] A. Widmer-Cooper, H. Perry, P. Harrowell, and D. R. Reichman, J.Chem.Phys. **131**, 194508 (2009).
[26] H. Zhang, D. J. Srolovitz, J. F. Douglas, and J. A. Warren, Proc. Natl. Acad. Sci. USA **106**, 7735 (2009).
[27] X. Xia and P. G. Wolynes, PNAS **97**, 2990 (2000).
[28] J. Dudowicz, K. F. Freed, and J. F. Douglas, Adv. Chem. Phys. **137**, 125 (2008).
[29] L. Larini, A. Ottochian, C. De Michele, and D. Leporini, Nature Physics **4**, 42 (2008).
[30] A. Ottochian, C. De Michele, and D. Leporini, J. Chem. Phys. **131**, 224517 (2009).
[31] F. Puosi and D. Leporini, J.Phys. Chem. B **115**, 14046 (2011).
[32] F. Puosi, C. D. Michele, and D. Leporini, J. Chem. Phys. **138**, 12A532 (2013).
[33] C. De Michele, E. Del Gado, and D. Leporini, Soft Matter **7**, 4025 (2011).
[34] A. Ottochian, F. Puosi, C. D. Michele, and D. Leporini, Soft Matter **9**, 7890 (2013).
[35] B. A. Pazmiño Betancourt, P. Z. Hanakata, F. W. Starr, and J. F. Douglas, Proc. Natl. Acad. Sci. USA, in press (2015).
[36] A. Ottochian and D. Leporini, J. Non-Cryst. Solids **357**, 298 (2011).
[37] A. Ottochian and D. Leporini, Phil. Mag. **91**, 1786 (2011).
[38] F. Puosi and D. Leporini, J. Chem. Phys. **136**, 211101 (2012).
[39] F. Puosi and D. Leporini, J. Chem. Phys. **136**, 041104 (2012).
[40] F. Puosi and D. Leporini, J. Chem. Phys. **136**, 164901 (2012).
[41] F. Puosi and D. Leporini, J. Chem. Phys. **139**, 029901 (2013).
[42] U. Buchenau and R. Zorn, Europhys. Lett. **18**, 523 (1992).
[43] L. Andreozzi, M. Giordano, and D. Leporini, J. Non-Cryst. Solids **235**, 219 (1998).
[44] M. T. Cicerone, Q. Zhong, J. Johnson, K. A. Aamer, and M. Tyagi, J. Phys. Chem. Lett. **2**, 1464 (2011).
[45] V. N. Novikov and A. P. Sokolov, Phys. Rev. Lett. **110**, 065701 (2013).
[46] P. A. Egelstaff, *An introduction to the liquid state* (Clarendon Press, Oxford, 1992), 2nd ed.
[47] J. P. Hansen and I. R. McDonald, *Theory of Simple Liquids, 3rd Ed.* (Academic Press, 2006).
[48] Note that $t^\star$ is one order of magnitude shorter than the times considered in ref. [23].
[49] G. Adam and J. H. Gibbs, J. Chem. Phys. **43**, 139 (1965).
[50] J. H. Gibbs and E. A. DiMarzio, J. Chem. Phys. **28**, 373 (1958).
[51] W. Götze, *Complex Dynamics of Glass-Forming Liquids: A Mode-Coupling Theory* (Oxford University Press, Oxford,

2008).
[52] K. Chen, E. J. Saltzman, and K. S. Schweizer, Annu. Rev. Condens. Matter Phys. **1**, 277 (2010).
[53] V. Lubchenko and P. G. Wolynes, Annu. Rev. Phys. Chem. **58**, 235 (2007).
[54] G. Tarjus, S. A. Kivelson, Z. Nussinov, and P. Viot, J. Phys.: Condens. Matter **17**, R1143 (2005).
[55] J. C. Dyre and W. H. Wang, J.Chem.Phys. **136**, 224108 (2012).
[56] D. Coslovich, Phys. Rev. E **83**, 051505 (2011).
[57] S. Capponi, S. Napolitano, and M. Wübbenhorst, Nat. Commun. **3**, 1233 (2012).
[58] S. Singh, M. D. Ediger, and J. J. de Pablo, Nat. Mater. **12**, 139 (2013).
[59] T. Speck, A. Malins, and C. P. Royall, Phys. Rev. Lett. **109**, 195703 (2012).
[60] A. Barbieri, G. Gorini, and D. Leporini, Phys. Rev. E **69**, 061509 (2004).
[61] G. M. Hocky, D. Coslovich, A. Ikeda, and D. R. Reichman1, Phys. Rev. Lett. **113**, 157801 (2014).
[62] J. C. Conrad, F. W. Starr, and D. A. Weitz, J. Phys. Chem. B **109**, 21235 (2005).
[63] C. P. Royall, S. R. Williams, T. Ohtsuka, and H. Tanaka, Nat. Mater. **7**, 556 (2008).
[64] M. Leocmach and H. Tanaka, Nat. Commun. **3**, 974 (2012).
[65] T. S. Jain and J. de Pablo, J.Chem.Phys. **122**, 174515 (2005).
[66] C. R. Iacovella, A. S. Keys, M. A. Horsch, and S. C. Glotzer, Phys. Rev. E **75**, 040801(R) (2007).
[67] N. C. Karayiannis, K. Foteinopoulou, and M. Laso, J. Chem. Phys. **130**, 164908 (2009).
[68] B. Schnell, H. Meyer, C. Fond, J. Wittmer, and J. Baschnagel, Eur. Phys. J. E **34**, 97 (2011).
[69] M. Asai, M. Shibayama, and Y. Koike, Macromolecules **44**, 6615 (2011).
[70] L. Larini, A. Barbieri, D. Prevosto, P. A. Rolla, and D. Leporini, J. Phys.: Condens. Matter **17**, L199 (2005).
[71] S.Sastry, T. Truskett, P. Debenedetti, S.Torquato, and F.H.Stillinger, Mol. Phys. **95**, 289 (1998).
[72] S. Bernini, F. Puosi, and D. Leporini, J. Non-Cryst. Solids **407**, 29 (2015).
[73] M. Sega, P. Jedlovszky, N. N. Medvedev, and R. Vallauri, J. Chem. Phys. **121**, 2422 (2004).
[74] D.Rigby and R. J. Roe, Macromolecules **23**, 5312 (1990).
[75] G. Ruocco, M. Sampoli, and R. Vallauri, J. Chem. Phys. **96**, 6167 (1992).
[76] J.-P. Shih, S.-Y. Sheu, and C.-Y. Mou, J.Chem.Phys. **100**, 2202 (1994).
[77] P. Jedlovszky, J. Chem. Phys. **111**, 5975 (1999).
[78] K. T. Wikfeldt, M. Leetmaa, A. Mace, A. Nilsson, and L. G. M. Pettersson, J. Chem. Phys. **132**, 104513 (2010).
[79] G. Stirnemann and D. Laage, J. Chem. Phys. **137**, 031101 (2012).
[80] Y. Liao, D. Lee, and P. He, Powder Technology **123**, 1 (2002).
[81] W. P. Krekelberg, V. Ganesan, and T. M. Truskett, J. Chem. Phys. **124**, 214502 (2006).
[82] J. C. G. Montoro and J. L. F. Abascal, J. Phys. Chem. **97**, 4211 (1993).
[83] C. Brito and M. Wyart, J. Stat. Mech.: Theory Exp. p. L08003 (2007).
[84] A. Lemaître, Phys. Rev. Lett. **113**, 245702 (2014).
[85] L. Berthier and R. L. Jack, Phys. Rev. E **76**, 041509 (2007).
[86] G. Mie, Annalen der Physik **316**, 657 (1903).
[87] F. Stacey, B. J. Brennan, and R. D. Irvine, Geophysical Survey **4**, 189 (1981).
[88] Y. Zhang, D. Zhao, R. Wang, and W. Wang, Acta Materialia **51**, 1971 (2003).
[89] G. A. Vliegenthart, J. F. M. Lodge, and H. N. W. Lekkerkerker, Physica A **263**, 378 (1999).
[90] M. Edalat, S. S. Lan, F. Pang, and G. A. Mansoori, Int. J. Thermophys. **1**, 177 (1980).
[91] A. Gil-Villegas, A. Galindo, P. J. Whitehead, S. J. Mills, G. Jackson, and A. N. Burgess, J. Chem. Phys. **106**, 4168 (1997).
[92] T. Lafitte, A. Apostolakou, C. Avendaño, A. Galindo, C. S. Adjiman, E. A. Müller, and G. Jackson, J.Chem.Phys. **139**, 154504 (2013).
[93] P. Chaudhuri, L. Berthier, and W. Kob, Phys. Rev. Lett. **99**, 060604 (2007).
[94] J. Baschnagel and F. Varnik, J. Phys.: Condens. Matter **17**, R851 (2005).
[95] G. S. Grest and K. Kremer, Phys. Rev. A **33**, 3628 (1986).
[96] H. C. Andersen, J. Chem. Phys. **72**, 2384 (1980).
[97] S. Nosé, J. Chem. Phys. **81**, 511 (1984).
[98] M. E. Tuckerman, B. J. Berne, and G. J. Martyna, J. Chem. Phys. **97**, 1990 (1992).
[99] K. Kremer and G. S. Grest, J. Chem. Phys. **92**, 5057 (1990).
[100] M. Kröger, Phys. Rep. **390**, 453 (2004).
[101] W. Paul and G. D. Smith, Rep. Prog. Phys. **67**, 1117 (2004).
[102] C. Luo and J.-U. Sommer, Comp. Phys. Comm. **180**, 1382 (2009).
[103] W. Kob and H. C. Andersen, Phys. Rev. Lett. **73**, 1376 (1994).
[104] S. S. Ashwin and S. Sastry, J.Phys.: Condens. Matter **15**, S1253 (2003).
[105] A. Barbieri, D. Prevosto, M. Lucchesi, and D. Leporini, J. Phys.: Condens. Matter **16**, 6609 (2004).
[106] R. Richert, J. Phys.: Condens. Matter **14**, R703 (2002).
[107] A. Ottochian, C. De Michele, and D. Leporini, Philosophical Magazine **88**, 4057 (2008).
[108] S. Bernini, F. Puosi, M. Barucco, and D. Leporini, J. Chem. Phys. **139**, 184501 (2013).
[109] A. Widmer-Cooper and P. Harrowell, J. Non-Cryst. Solids **352**, 5098 (2006).
[110] K. L. Ngai, L.-R. Bao, A. F. Yee, and C. L. Soles, Phys. Rev. Lett. **87**, 215901 (2001).
[111] S. Arizzi, P. H. Mott, and U. W. Suter, J. Polym. Sci.: Part B: Polymer Physics **30**, 415 (1992).
[112] L. Bøhling, A. A. Veldhorst, T. S. Ingebrigtsen, N. P. Bailey, J. S. Hansen, S. Toxvaerd, T. B. Schrøder, and J. C. Dyre, J. Phys.: Condens. Matter **25**, 032101 (2013).
[113] J. P. Boon and S. Yip, *Molecular Hydrodynamics* (Dover Publications, New York, 1980).